Resonance Raman spectroscopy of NADH, NAD+, ferredoxin and cytochrome c in Sporomusa ovata and Clostridium carboxidivorans for

Vibrational Spectroscopy 143 (2026) 103895

Contents lists available at ScienceDirect

Vibrational Spectroscopy

journal homepage: www.elsevier.com/locate/vibspec

Resonance Raman spectroscopy of NADH, NAD^+ , ferredoxin and cytochrome c in *Sporomusa ovata* and *Clostridium carboxidivorans* for microbial electrosynthesis applications

Adolf Krige [a], Ulrika Rova [b], Paul Christakopoulos [b], Lisbeth Olsson [a], Kerstin Ramser [c,*]

[a] Industrial Biotechnology, Life Sciences, Chalmers University of Technology, Sweden
[b] Department of Civil, Environmental and Natural Resources, Luleå University of Technology, Sweden
[c] Department of Engineering Sciences and Mathematics, Luleå University of Technology, Sweden

ARTICLE INFO

Keywords:
Microbial electrosynthesis
Resonance Raman spectroscopy
Biomarkers
Sporomusa ovata
Clostridium carboxidivorans

ABSTRACT

Microbial electrosynthesis (MES) offers a sustainable alternative for the production of platform chemicals from CO_2. Label-free Raman spectroscopy can provide direct insights into biomolecular changes in MES, reflecting metabolic activity and production. In this study defined co-cultures of electro-active bacteria, i.e. *Sporomusa ovata* and *Clostridium carboxidivorans,* were investigated by confocal resonance Raman micro-spectroscopy tuned to 532 nm to gain insights into the microbial processes of biomarkers involved in the Wood-Ljundahl pathway. The results were correlated to high-performance liquid chromatography (HPCL) and optical density measurements regarding the production rate of acetate, butyrate, ethanol and butanol. Pre-processed difference Raman spectra of co-cultures from *S. ovata* and *C. carboxidivorans* at ratios 1:10, 10:1, and 1:1 were compared to monocultures on day 1 and 2, revealing substantial variations in Raman intensity and thus the relative metabolic activity of NADH, NAD^+, ferredoxin and cytochrome c. Such information may point to high metabolic activity at the start of acetate, butyrate, ethanol, and butanol production followed by a steady state at day four. This was verified by Raman difference spectra between fresh cultures and $>$ 4 days old cultures, indicating a similar degree of metabolic activity after a certain time during ongoing production. Interestingly, the Raman spectra did not reveal any differences in metabolism depending on feedstocks, i.e. CO_2 and H_2 versus betaine or different ratios of co-cultures that were significantly more productive. This qualitative study demonstrates that resonance Raman spectroscopy is a viable tool for metabolic investigations of microbial electrosynthesis systems with potential for *in situ* investigations.

1. Introduction

Despite actions against global warming, anthropogenic emissions keep increasing due to population growth and growing prosperity, which calls for a capture, reduction and/or reutilization of CO_2. Bioelectrical systems employing microbial electrosynthesis (MES), microbial electrolysis, or electro methanogenesis are suitable promising candidates as they generate chemicals and fuels from CO_2 [1]. Hitherto, MES are limited by poor selectivity, low production rates as well as complex microbial interactions and metabolic mechanisms that are not yet fully understood [2]. One promising approach to improve MES productivity is the use of co-cultures of different microorganisms rather than relying on one single species. The synergy and cooperation of co-cultures can lead to higher productivities and yields [3]. Here, we focus on *Sporomusa ovata* and *Clostridium carboxidivorans*. *S. ovata* is one of the earliest known organisms capable of acetogenesis via MES [4,5], while *C. carboxidivorans* has been shown to produce acetate via the Wood-Ljungdahl pathway. Co-cultures have been shown to be surprisingly effective in boosting electron transfer, and subsequent production. For example, a co-culture of *C. tyrobutyricum* and *C. ljungdahlii* was shown to enhance carbon recovery and butyrate production, where *C. tyrobutyricum* produced CO_2 and H_2 during sugar fermentation, which could subsequently be converted to acetate by *C. ljungdahlii* via the Wood-Ljungdahl pathway, followed by conversion of excess acetate to butyrate by *C.* tyrobutyricum [6]

NADH and reduced ferredoxin (Fd) play a pivotal role in the

* Corresponding author.
E-mail address: kerstin.ramser@ltu.se (K. Ramser).

https://doi.org/10.1016/j.vibspec.2026.103895
Received 10 October 2025; Received in revised form 23 January 2026; Accepted 11 February 2026
Available online 12 February 2026

Table 1
Raman band assignment [13–15].

Raman band [cm^{-1}]	Assignment
1676	cyt c oxidized
1664	Amide I
1630	NADH/NAD^+
1587	cyt c oxidized/reduced
1560	NAD^+
1550	cyt c oxidized
1505	NADH/NAD^+
1501	cyt c oxidized
1448	lipids
1410	NADH/NAD^+
1330	NAD^+
1314	cyt c oxidized/reduced
1305	NADH
1250	Amide I & II
1130	cyt c oxidized/reduced
1020	NADH
1004	phenylalanine
969	cyt c oxidized
824	tyrosine
750	cyt c reduced
720	NADH/NAD^+
625	oxidized Ferredoxin

reduction of CO_2 via the Wood-Ljungdahl pathway, as well as in the chain elongation of acetyl-CoA to butyrate and butanol. This pathway requires high reducing power, especially to enable the conversion of acetyl-CoA into more valuable, longer-chain carbon products, like butanol. Hydrogenases play a key role in this context, by oxidizing H_2 to generate the reducing equivalents (i.e., reduced ferredoxin and NADPH) for the Wood-Ljungdahl pathway. There are two main classes of hydrogenases: [FeFe]-hydrogenases, which have a catalytic bias toward H_2 production, and [NiFe]-hydrogenases, which act primarily as H_2 oxidation catalysts [7].

S. ovata and *C. carboxidivorans* co-cultures have shown to produce higher titres of ethanol and butanol than the mono-cultures. The exact mechanism for this is not yet known, but is most likely due to the higher hydrogen uptake rate of *S. ovata* (up to six times higher), followed by some degree of metabolic cross-feeding or interspecies electron transfer [8].

Based on genomic data, both *S. ovata* and *C. carboxidivorans* are predicted to contain five distinct hydrogenases; with *C. carboxidivorans* containing a single gene encoding a [Ni-Fe]-hydrogenase; whereas *S. ovata* contains three genes encoding [Ni-Fe]-hydrogenases [9,10]. The improved H_2 of *S. ovata* and subsequent improved alcohol production can most likely be ascribed to greater abundance of [Ni-Fe]-hydrogenases. This improved hydrogenase activity should lead to an increase in NADH and reduced ferredoxin. Because many key steps in anaerobic fermentation are NADH-dependent, an increased NADH/-NAD^+ ratio pushes metabolism toward more reduced end-products such as ethanol and butanol [11].

Recent advances in the field of environmental and catalytic systems have shown that spectroscopic techniques possess distinct advantages in capturing electron redistribution and bonding evolution during complex multi-field driven reactions. For instance, a recent study by Cheng et. al. investigates wastewater purification using a CdZnS interface that combines ultrasound-assisted-treatment and photocatalysis for enhanced removal of toxic Azo dyes used in textiles, cosmetics and leather products [12]. Several microscopic and spectroscopic tools were used with promising results, among them Fourier-Transform Infrared (FT-IR) spectroscopy. Efficient Azo dye removal was achieved through adsorption on the CdZnS, and reactive oxygen dye degradation through the piezoelectric effect of the CdZnS. The FT-IR spectrum revealed CR adsorption by the increase of the S═O stretching mode and hydrogen bond formation at the CdZnS-CR interface. Inspired by this study, the aim here was to qualitatively investigate the feasibility of resonance Raman spectroscopy to interrogate the metabolic interplay of the Wood-Ljungdahl pathway of *S. ovata* and *C. carboxidivorans*, cultured both as monocultures and as co-cultures at different ratios using different feedstocks. The results were compared to high-performance liquid chromatography (HPCL) and optical density measurements that showed the growth rate of the bateria and production rate of platform products. Resonance Raman spectroscopy has been applied since the 1980s to investigate the redox states of NADH, NAD^+, as well as the c-type cytochromes (cyt c) [13,14]. Furthermore, a resonance Raman spectroscopic investigation of the oxidized state of Fd showed Raman bands in the low wavenumber region up to 900 cm^{-1} using 406.7 nm, 457.9 nm or 514.5 nm as excitation wavelengths, while the reduced state was only accessible using 568.2 nm laser light to generate rather weak Raman bands up to 400 cm^{-1} [15]. Inspired by these early studies and our previous work where the redox state of cyt c was monitored online and *in situ* [16], we here investigated the possibility to monitor variations in metabolism of NADH, NAD^+, cyt c, and oxidized Fd in monocultures and co-cultures of *S. ovata* and *C. carboxidivorans*. Raman spectral information may give insights to the microbial metabolic activities in MES applications and provide knowledge for process improvement.

2. Material and methods

2.1. Microbes, media, and cultivation

Cultures of *S. ovata* and *C. carboxidivorans* were prepared by inoculating pre-cultures from a frozen stock directly into 50 mL of anaerobic medium (described below) using fructose as carbon source. The pre-cultures and final co-cultures were grown in a modified *Clostridium* growth medium. *S. ovata* was unable to grow in Turbo CGM due to its low sodium content, therefore *S. ovata* monocultures and co-cultures were supplemented with 1.25 g/L NaCl. Additional 1.25 g/L NaCl was also supplemented to *C. carboxidivorans* to enable comparison of the results. The medium was based on the Turbo *Clostridium* Growth Medium (Turbo CGM) [17]. The final medium consisted of: 1.25 g/L KH_2PO_4, 0.25 g/L K_2HPO_4, 1 g/L (2.25 g/L for *S. Ovata* cultures) NaCl, 0.01 g/L $MnSO_4$, 0.348 g/L $MgSO_4$, 0.01 g/L $FeSO_4$, 1 g/L yeast extract, 1 g/L $(NH_4)_2SO_4$, 2 g/L sodium acetate, 0.02 g/L $CaCl_2{\cdot}2\ H_2O$, 0.50 mL/L sodium resazurin stock (0.1 % w/v), 0.2 mL/L of a stock containing Na_2SeO_3 (0.05 mM) and Na_2WO_4 (1 g/L), 1 mL/L trace element solution (sl-10), and 10 mL/L vitamin solution. The medium was sparged with 100 % N_2 and 50 mL was aliquoted into 100-mL serum vials before being autoclaved. The following stocks were then added just before use: 0.5 mL/50 mL $NaCO_3$ (10 %) and 0.5 mL/50 mL L-Cysteine-HCl × H_2O (3 %). To ensure sufficient biomass for the inoculum, all pre-cultures were grown using 5 g/L fructose. Fructose as carbon source was added from a filter-sterilized stock for the inoculums.

To ensure a consistent substrate supply, the gas in the serum vials was exchanged via an in-house gas exchanger, that alternates 4 cycles of vacuum followed by an 80:20 H_2:CO_2 gas mixture at 1 bar in each exchange cycle. For initial screening of cultures, the serum vials were run as a batch fermentation, with only a single exchange of the headspace in the serum vials, and no additional carbon source was provided. The subsequent optimization experiments were run as a fed-batch fermentation by exchanging the headspace daily with the 80:20 H_2:CO_2 gas mixture at 1 bar, in order to ensure that there was no substrate limitation.

The serum vials were inoculated to an optical density at 600 nm (OD_{600}) of 0.05 using the equations below:

$$V_{tot}C_{tot} = (V_1C_1 + V_2C_2)$$

$$C_{tot} = \frac{V_1C_1 + V_2C_2}{50\text{mL} + V_1 + V_2} = 0.05$$

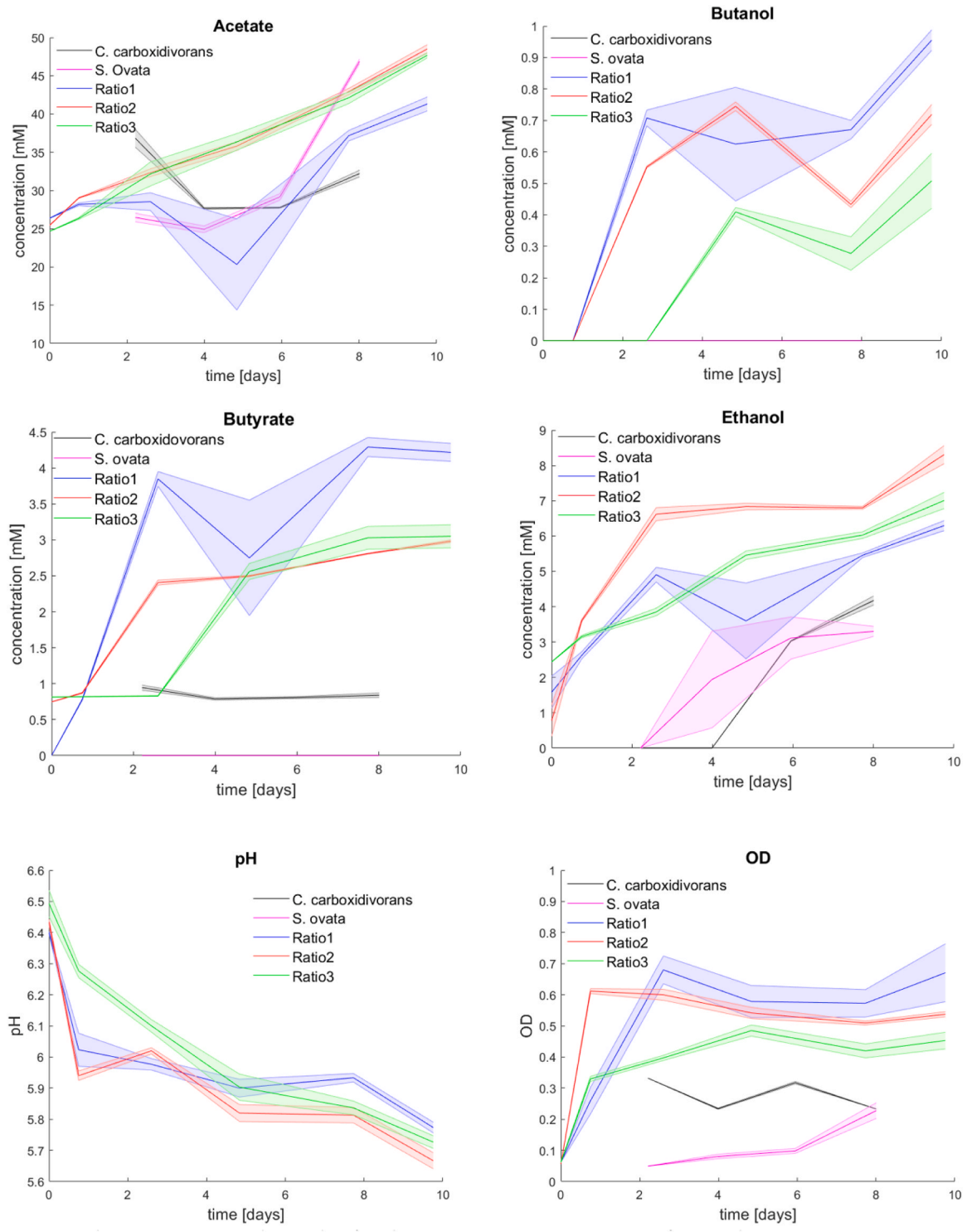

Fig. 1. The upper rows show the final product concentrations of C. carboxidivorans and S. ovata monocultures, as well as that of the co-culture at different inoculation ratios according to the legends. The Ratios S. ovata:C. carboxidivorans equal; ratio 1 = 10:1, ratio 2 = 1:1 and ratio 3 = 1:10. Below the influence of pH and OD can be seen for all cultures.

where V_1 and V_2 are the volumes of the co-cultures injected, and C_1 and C_2 are the OD_{600} values of the inoculi just before inoculation.

The serum vials were then grown for approximately 10 days in a shaker incubator at 37°C, and sampled periodically for high-performance liquid chromatography (HPLC) and OD_{600} measurements.

2.2. Analytical measurements

Samples of 0.6 mL were taken using a 1-mL syringe and 25 G needle and subsequently split for OD_{600} and HPLC analysis. OD_{600} was measured in a 96-well microplate using 200-µL samples and milli-Q water as a blank (SPECTROstar nano, Ortenberg, Germany).

For HPLC, all samples were filtered through a 96-well microplate filter and analyzed on an LC-4000 instrument (JASCO, Easton, MD,

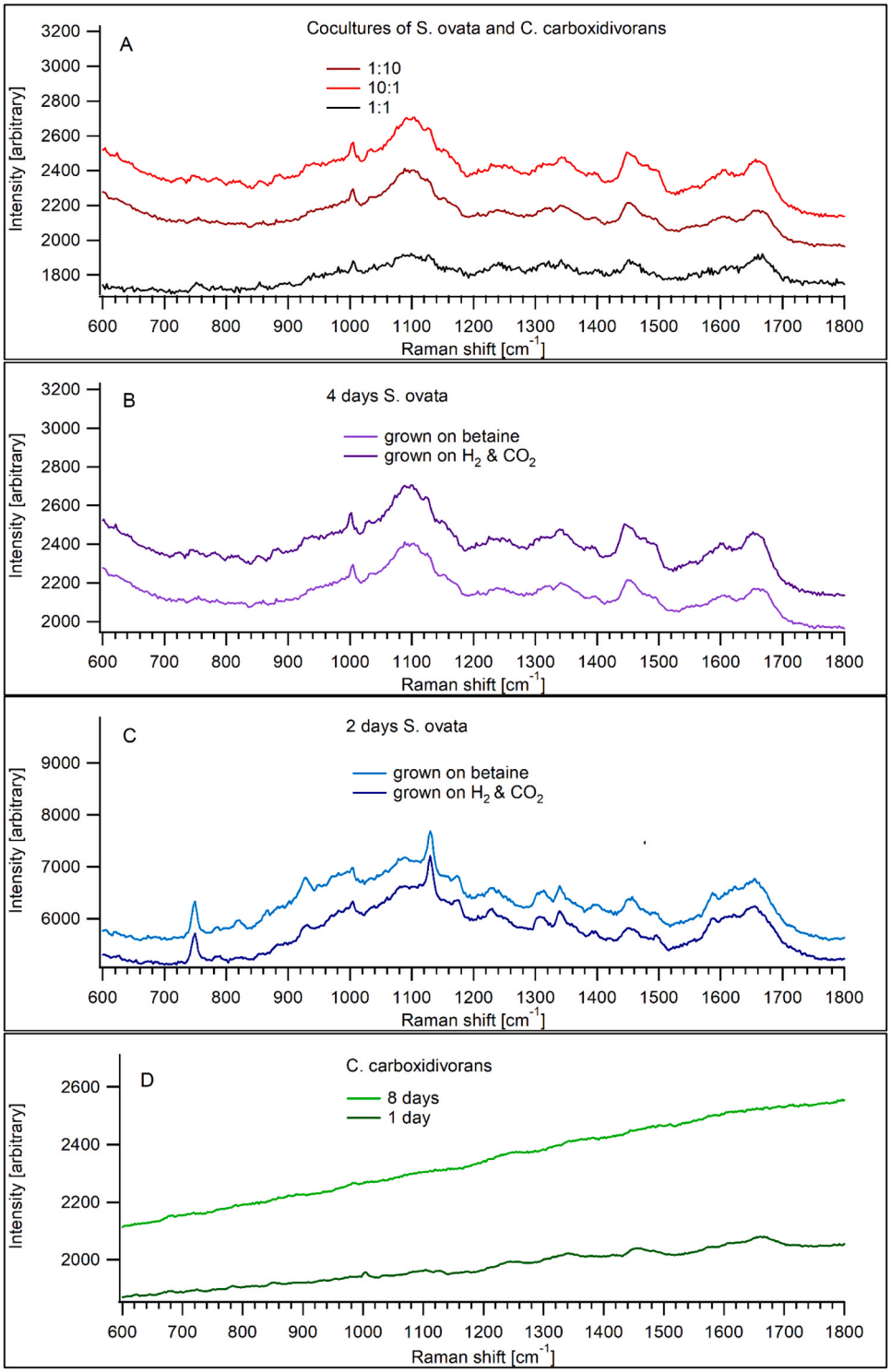

Fig. 2. Panel A: co-cultures of S. ovata and C. carboxidivorans at different ratios (dark red - 10:1, red - 1:10, black - 1:1). Panel B: S. ovata after 4 days of growth on betaine (dark purple) or on CO_2 and H_2 (light purple). Panel C: S. ovata after 2 days of growth growth under the same conditions as in Panel B. Panel D: C. carboxidivorans grown for 8 days (light green) and 1 day (dark green).

USA), equipped with a refractive index detector and a Rezex ROA-Organic Acid H^+ Ion Exclusion HPLC Column (Phenomenex, Torrance, CA, USA). The column was maintained at 60°C, and 5 mM H_2SO_4 was used as mobile phase at a flow rate of 0.6 mL/min.

To determine the fraction of *S. ovata* and *C. carboxidivorans*, co-cultures were profiled using 16S ribosomal RNA sequencing (Eurofins Genomics, Ebersberg, Germany). DNA extraction and library preparation were carried out by Eurofins Genomics using the 16S V3-V5 amplicon. Raw sequencing data and detailed microbiome profiling are available upon request.

2.3. Confocal resonance Raman measurements

All samples were taken under anaerobic conditions and concentrated via centrifuging 15 mL and resuspending the cell pellet in 1 mL spent medium. The concentrated samples were then pipetted onto a

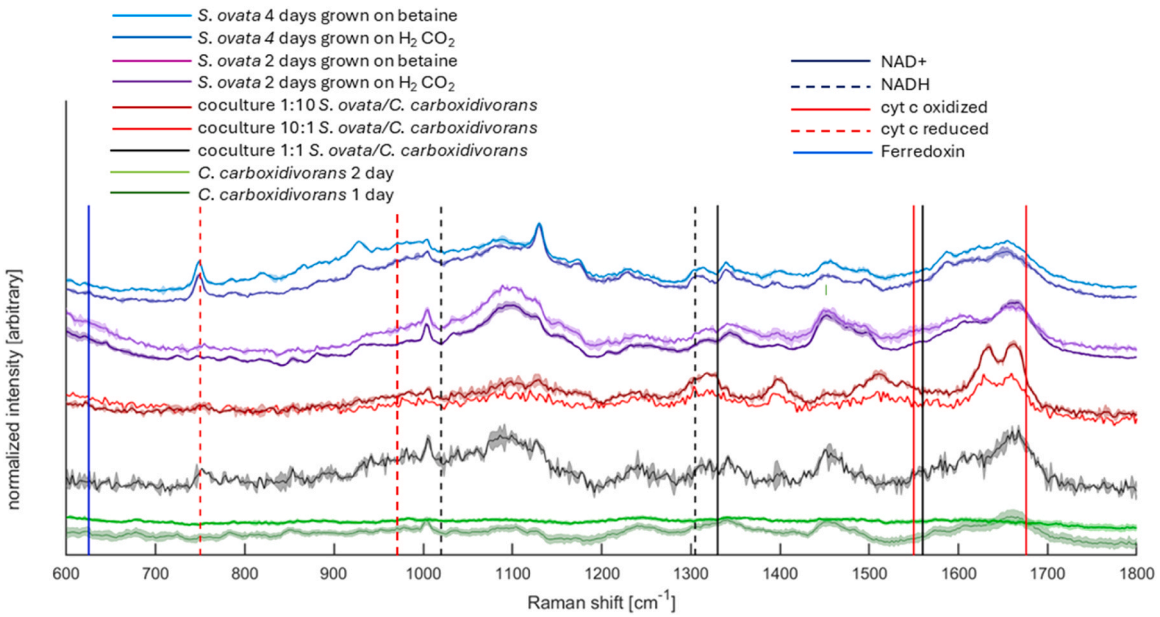

Fig. 3. Background reduced and normalized Raman spectra colour coded according to the legend to the left. The standard deviation is given to highlight the trend of the data. The vital metabolic Raman bands for NADH, NAD^+, cyt c in the reduced and oxidized forms are highlighted with vertical lines according to the legend to the right and Fd in the reduced form is highlighted by the blue vertical line.

microscope slide (approximately 20 μL). To maintain anaerobic conditions, the edges of the cover slide was coated in Petroleum jelly (Vaseline) by first spreading the Vaseline thinly on a microscope slide to then scrape the edges of the cover slide over the Vaseline covered microscope slide. The sealed samples were placed in a 50 mL Falcon tube and sealed anaerobically until just before measurement.

Raman spectra were taken using a confocal WITec alpha300 R Raman microscope (WITec GmbH, Ulm, Germany) using a green laser (532 nm) set to 4 mW at an integration time of 20 × 2 s using a 20 × microscope objective. Measurements were taken at slightly different locations to get an average of the sample. A minimum of 20 spectra were taken per sample, of these good quality spectra were selected after discarding Raman spectra with high influence of glass interference or poor signal to noise ratio. *C. carboxidivorans* exposed a high signal to noise ratio and fluorescence and 18 and 14 spectra were evaluated for each sample. Coculture 1:10 only had one good spectrum and S. ovata 4 days grown with H_2 and CO_2 had 3 good quality spectra, from the rest 2 spectra were selected.

2.4. Treatment of Raman spectra and assignment of Raman bands

A number of consecutive preprocessing steps were applied to the raw spectra. For the difference Raman spectra smoothing was employed using Eilers' algorithm with $d = 2$ and $\lambda = 10$ [18]. The background was subtracted by fitting a piecewise polynomial to each spectrum [19]. The spectra were vector normalized so the integrated intensities were equalized. Means of the pre-processed spectra were taken for *C. carboxidivorans* day 1, and day 4. Difference spectra were taken to investigate the grade of differences in metabolism, e.g. monocultures minus different cocultures, age or different feedstocks. The Raman bands were assigned using references [13–15], see Table 1.

The Raman bands highlighted by different colours in Table 1 were used to investigate the metabolic activity of the bacteria. They belong to strong or medium strong Raman bands from Fd, cyt c in the reduced and oxidized form, and NADH & NAD^+.

3. Results and discussions

Fig. 1 shows the final product concentrations (mM) of *C. carboxidivorans* and *S. ovata* monocultures, as well as those of co-cultures at different inoculation ratios over ten days. The ratios of *S. ovata/C. carboxidivorans* equal; ratio 1 = 10:1, ratio 2 = 1:1 and ratio 3 = 1:10. Notably, *S. ovata* did not produce any butyrate, but with an increasing amount of *C. Carboxidivorans*, the production rate increased. None of the monocultures produced butanol. In all cases, the co-cultures were more productive than the monocultures.

Fig. 2 shows raw Raman spectra of *S. ovata* an *C. carboxidivorans*, either in mono or in different co-cultures with H_2 and CO_2 as sole electron and carbon sources.

The raw data, was pre-processed, normalized, and cropped to the fingerprint region (Fig. 3). Here the vital targeted important compounds, i.e., NADH, NAD^+, cyt c and Fd, for microbial electrosynthesis are depicted by the vertical coloured lines. Other peaks from proteins, lipids and amino acids are not specified.

Note that the treated Raman spectrum of *C. carboxidivorans* after two days shows a straight line due to the high intrinsic fluorescence of this sample that overshadows the Raman signal. From now on, this measurement series is excluded. However, the high fluorescence might indicate laser induced fluorescence (LIF) that can be triggered if NADH and NAD^+ are highly abundant and active.

It is further evident that the obligate anaerobe *S. ovata* shows clear cyt c features, which also appear – though to a less extent - in the co-cultures and in 4-days old samples. Note that *S. ovata* and the 1:1 co-culture show the highest signatures of reduced cyt c at 750 cm^{-1}. C-type cytochromes are typically involved in electron transport for cellular respiration, yet is also crucial for electron transfer, particularly in bacteria like Shewanella and Geobacter, where they shuttle electrons to external, non-oxygen terminal electron acceptors such as fumarate, nitrate, or insoluble metal oxides [20]. The finding of cyt c here is in accordance with our previous work [16]. The role of cyt c in CO_2 reduction remains unclear, yet *S. ovata* is known to produce cyt c, which is important for the translocation of electrons during nitrate reduction. Further, proteomics data has shown that of cyt c production in *S. ovata* is upregulated during nitrate metabolism, but not when CO_2 and H_2 are used as the sole electron and carbon sources [21]. These findings need more investigation.

More information can be retrieved from the difference spectra, see Fig. 4. For clarity and due to the small amount of samples the standard

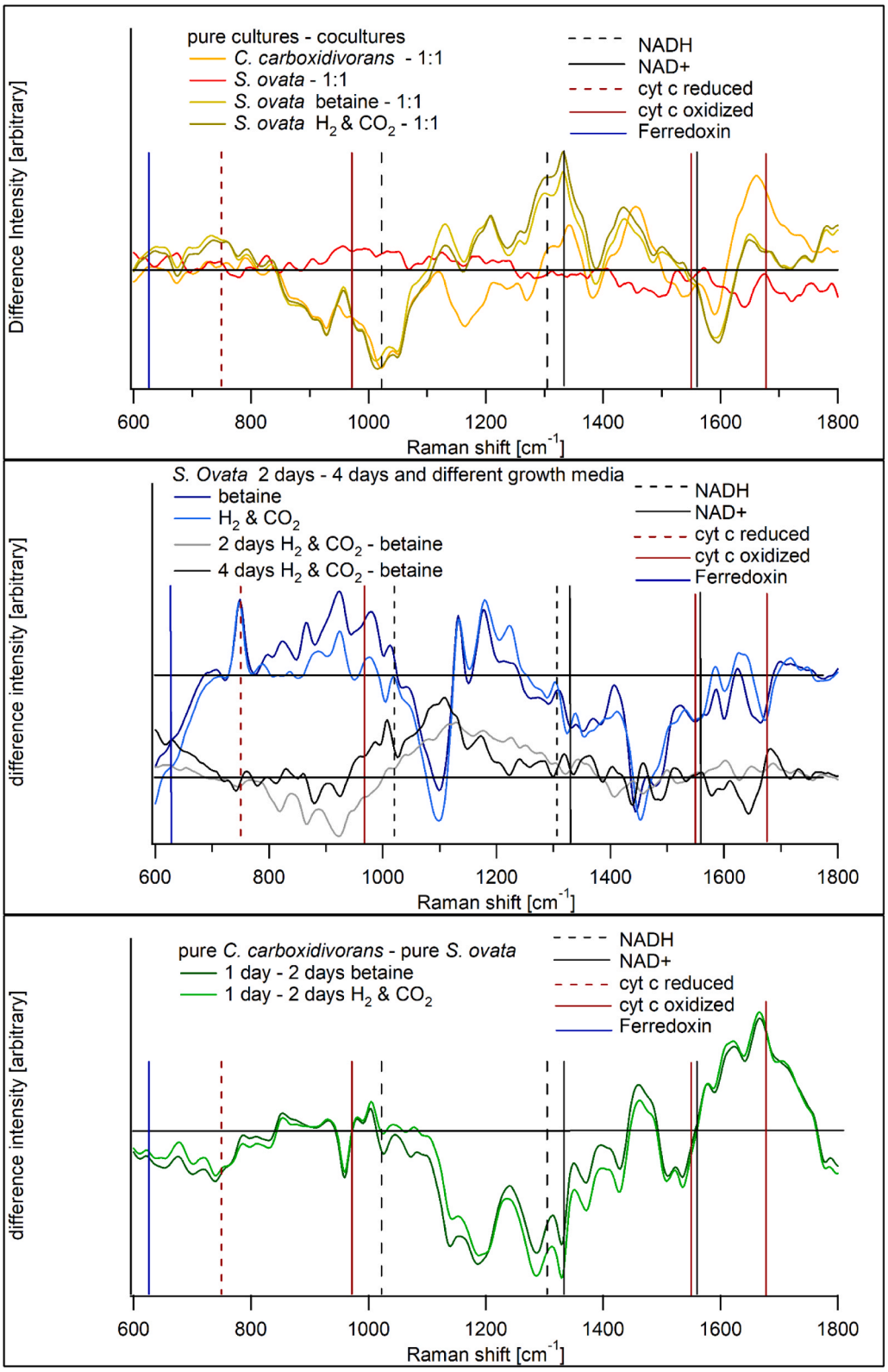

Fig. 4. Difference spectra according to the insert on the left-hand side. The Raman bands for NADH, NAD^+, and cyt c in the reduced and oxidized form, and oxidized Fd are depicted according to the legend on the right-hand side The zero lines for all difference spectra are the horizontal dark grey lines.

deviation is left out. When the difference spectrum is close to the horizonal zero line, the spectral Raman signatures of the biomarkers highlighted in Table 1 are equal between the two compared spectra. Values above this line indicates that the relative intensity of this biomolecular Raman signature in the denominator is higher and below indicates less, which may indicate a difference in metabolism or abundance of the biomolecule.

The uppermost graph of Fig. 4 show the difference spectra between *S. ovata* fed on betaine or H_2 and CO_2 minus the 1:1 co-culture in kaki and in brown respectively, while the difference spectrum of

C. carboxidivorans is shown in orange. There is quit a strong difference in the relative concentration of NADH, NAD^+ in both the reduced and oxidized form of the monocultures of either *C. carboxidivorans* or *S. ovata* when compared to the co-cultures, with the co-cultures showing a higher abundance and activity of the selected biomarkers. The relative increase of activity in NADH and NAD^+ may indicate a greater reducing potential in the co-cultures, which could support a higher CO_2 metabolism. This clearly points towards a synergistic effect of co-cultures, which is clearly beneficial for MES. Furthermore, the oxidised Raman band of Fd (blue striped line) appears lower in the co-culture samples. This could imply, even if it is not visible in the presented Raman data, that a greater percentage of the available Fd is in a reduced state, which would contribute to a greater reducing potential. These two observations might be evidence of synergistic behaviour between the organisms in the co-cultures, resulting in higher reducing power, and a subsequent increase in reduced products, as observed in the increase ethanol and butanol levels in the co-cultures (Fig. 1).

The lowest graph in Fig. 4 shows the difference spectrum of *C. carboxidivorans* minus *S. ovata* fed on betaine (dark green) and *C. carboxidivorans* minus *S. ovata* fed on CO_2 and H_2 (light green). There is a significant difference in the NADH, NAD^+ Raman bands, in both reduced and oxidized forms, when comparing the monocultures of *C. carboxidivorans* (1 days old) with *S. ovata* (2 days old). The relative decrease of NADH and NAD^+ may indicate a decreased reducing potential, which could lead to a lower CO_2 metabolism, either caused by the culture age or by type of bacteria. This may again indicate that *S. ovata* and *C. carboxidivorans* have quit opposite metabolic features. Notably, the difference spectra are otherwise quite similar, indicating that the feedstock does not strongly influence the data. This is further confirmed by the middle graph showing difference spectra between H_2 - betaine from 2 days old *S. ovata* (black) versus 4 days old *S. ovata* (grey) that both align close to the zero line. Age, however, seems to have a significant effect on the metabolism which can be seen in the dark and light blue difference spectra of *S. ovata*. Here, the reduced cyt c content at 750 cm^{-1} increases, while the oxidised cyt c at 1676 cm^{-1} also increases. Furthermore, NADH also seems to decrease, suggesting that the reducing potential levels out over several days of production. Differences between the two species can be traced in the cyt c content, since *C. carboxidivorans* lacks this protein. Overall, *S. ovata* appears to produce more NADH and seems to have a more active metabolism at this stage and under these conditions.

Microbial profiling confirmed that *C. carboxidivorans* grew significantly faster than *S. ovata* during the initial stages of the co-culture, reaching a fraction of above 80 % during the first day, despite a 1:1 inoculation ratio. However, between 1 and 5 days *S. ovata* started outcompeting *C. carboxidivorans*, with the fraction of *S. ovata* tripling, reaching a relative microbial fraction of above 35 % by day 5, which may be explained by the superior H_2 uptake, and possibly a higher metabolic production rate, especially at lower partial pressure of H_2.

The difference spectrum of *S. ovata* grown on either betaine or H_2 and CO_2, 2 days old (grey), and the 4 days old (black) seen below in the middle graph of Fig. 4 show practically no difference at all regarding the chosen biomarkers. This indicates that feedstock had no detectable effect on the biomolecular content at the same culture age, suggesting a consistent metabolic production regardless of feedstock. The same observation applies for the different ratios of the co-cultures, red spectrum in the uppermost graph. However, this might be because *C. carboxidivorans* grew significantly faster than *S. ovata* during the first day, which may result in a similar cell distribution, independent of the inoculation ratio. The changes are minor and not related to the NADH, NAD^+ or oxidized/reduced cyt c.

Culture age seems to have a levelling effect on the relative concentration of the discussed biomarkers, specifically cyt-c. The difference spectra between different days of the cultures (blue spectra seen at the top of the middle graph in Fig. 4), show big differences in cyt c metabolism, which seems to decrease after 4 days. This may indicate the levelling out of cell growth, which can be seen in the OD values in Fig. 1. In co-cultures, the specific growth rate is highest during the first day, and stabilizes around day 5, reaching a maximum OD of approximately 0.6.

4. Conclusions

Motivated by the recent study of Cheng et. al. [12], and previous work in our group [1,16], the aim of this study was to investigate the microbial metabolic activities of *S. Ovata* and *C. carboxidivorans*, with a particular focus on the Wood-Ljungdahl pathway, using resonance Raman spectroscopy. Difference resonance Raman spectra between *S. ovata*, *C. carboxidivorans* and co-cultures showed rather large variations in the difference spectrum, suggesting high metabolic activity in the start of acetate, butyrate, ethanol, and butanol production.

Higher NADH and NAD^+ activity in the co-cultures could be evidence of a synergistic effect, which allows the production of the more reduced products butyrate, ethanol, and butanol, which were not observed in the monocultures. There is also a rather large difference in metabolic activity between fresh and older than 4 days cultures, which may indicate the onset of a steady state, as cell concentration remained constant despite continued production of acetate, butyrate and ethanol. The Raman spectra did not reveal any differences in metabolic production regarding different feedstocks, i.e. CO_2 and H_2 versus betaine. Likewise, different ratio of co-cultures did not reveal any strong differences in metabolic activity. This may reflect that cultures had reached a steady state or that their respective metabolism were relatively similar under the conditions studied.

Overall, resonance Raman spectroscopy is a potential and valuable tool to investigate differences in the metabolic production of MES. Future studies should further explore the role of cyt c and extend the analysis to longer culture durations. In addition, examining Raman spectra at different pH levels could help identify optimal conditions for targeted metabolic pathways, since product selectivity strongly depends on the applied pH profile during cultivation.

CRediT authorship contribution statement

Ramser Kerstin Christina: Writing – original draft, Visualization, Validation, Methodology, Investigation, Funding acquisition, Formal analysis, Conceptualization. **Paul Christakopoulos:** Writing – review & editing, Supervision, Funding acquisition. **Lisbeth Olsson:** Writing – review & editing, Supervision, Project administration, Funding acquisition, Conceptualization. **Ulrika Rova:** Writing – review & editing, Funding acquisition, Conceptualization. **Adolf Krige:** Writing – review & editing, Visualization, Software, Investigation, Funding acquisition, Formal analysis, Data curation, Conceptualization.

Declaration of Competing Interest

All authors declare that there is no Conflict of Interest regarding the manuscript “Resonance Raman spectroscopy of NADH, NAD+ , ferrodexin and cytochrome c in *Sporosum ovata* and *Clostridium carboxidivorans* for microbial electrosynthesis applications”.

Acknowledgement

This work was fundend by the Swedish Energy Agency (P50578–1) and the Swedish Research Council (2022-03378). We would also like to thank the Chalmers Material Analysis Laboratory, Physics at Chalmers University of Technology, Gothenburg, Sweden, for access and tutoring to the Raman microscope.

Data availability

Data will be made available on request.

References

[1] S. Bajracharya, A. Krige, L. Matsakas, U. Rova, P. Christakopoulos, Advances in cathode designs and reactor configurations of microbial electrosynthesis systems to facilitate gas electro-fermentation, Bioresour. Technol. 354 (2022) 127178, https://doi.org/10.1016/j.biortech.2022.127178.

[2] F. Harnisch, J.S. Deutzmann, S.T. Boto, M.A. Rosenbaum, Microbial electrosynthesis: opportunities for microbial pure cultures, Trends Biotechnol. 42 (2024) 1035–1047, https://doi.org/10.1016/j.tibtech.2024.02.004.

[3] M.A. Rosenbaum, C. Berger, S. Schmitz, R. Uhlig, Microbial electrosynthesis i: Pure and defined mixed culture engineering. Advances in Biochemical Engineering/ Biotechnology, Springer Science and Business Media Deutschland GmbH, 2017, pp. 181–202, https://doi.org/10.1007/10_2017_17.

[4] K.P. Nevin, S. a Hensley, A.E. Franks, Z.M. Summers, J. Ou, T.L. Woodard, O. L. Snoeyenbos-West, D.R. Lovley, Electrosynthesis of organic compounds from carbon dioxide is catalyzed by a diversity of acetogenic microorganisms, Appl. Environ. Microbiol. 77 (2011) 2882–2886, https://doi.org/10.1128/AEM.02642-10.

[5] K.P. Nevin, T.L. Woodard, A.E. Franks, Z.M. Summers, D.R. Lovley, Microbial electrosynthesis: Feeding microbes electricity to convert carbon dioxide and water to multicarbon extracellular organic compounds, mBio 1 (2010) 1–4, https://doi.org/10.1128/mBio.00103-10.

[6] Wenchao Li, Chi Cheng, Jiaqi Zhao, Qian Li, Min Liu, Chaojun Wang, Chuang Xue, Enhanced carbon recovery and butyrate production in cocultivation of clostridium tyrobutyricum and c. ljungdahlii, XueACS Sustain. Chem. Eng. 12 (35) (2024), https://doi.org/10.1021/acssuschemeng.4c04373.

[7] P.F. Di Leonardo, G. Antonicelli, V. Agostino, A. Re, Genome-scale mining of acetogens of the genus clostridium unveils distinctive traits in [FeFe]- and [NiFe]-hydrogenase content and maturation, Microbiol. Spectr. 10 (2022) e01019-22, https://doi.org/10.1128/spectrum.01019-22.

[8] L. Muñoz-Duarte, S. Chakraborty, L.V. Grøn, M.F. Bambace, J. Catalano, J. Philips, H2 consumption by various acetogenic bacteria follows first-order kinetics up to H2 saturation, (2024) 2024.05.08.593002. https://doi.org/10.1101/2024.05.08.593002.

[9] J. Madjarov, R. Soares, C.M. Paquete, R.O. Louro, Sporomusa ovata as catalyst for bioelectrochemical carbon dioxide reduction: a review across disciplines from microbiology to process engineering, Front. Microbiol. 13 (2022). ⟨https://www.frontiersin.org/articles/10.3389/fmicb.2022.913311⟩.

[10] P.F. Di Leonardo, G. Antonicelli, V. Agostino, A. Re, Genome-scale mining of acetogens of the genus clostridium unveils distinctive traits in [FeFe]- and [NiFe]-hydrogenase content and maturation, Microbiol. Spectr. 10 (2022), https://doi.org/10.1128/spectrum.01019-22.

[11] Y. Yu, Z. Shi, W. Li, M. Bian, C. Cheng, Y. Xi, S. Yao, X. Zeng, Y. Jia, Application of exogenous electron mediator in fermentation to enhance the production of value-added products, Appl. Environ. Microbiol. 91 (2025), https://doi.org/10.1128/aem.00495-25.

[12] W. Li, C. Cheng, J. Zhao, Y. Song, C. Xue, Angew. Chem. Int. Ed. 64 (2025) e202425508, https://doi.org/10.1002/anie.202425508.

[13] T.W. Barett, pH-induced Modification of NAD and NADH Solutions Detected by Raman Spectroscopy, J. Raman Spectrosc. 9 (2) (1980) 130–133, https://doi.org/10.1002/jrs.1250090212.

[14] S. Hu, I.K. Morris, J.P. Singh, K.M. Smith, T.G. Spiro, Complete assignment of cytochrome c resonance raman spectra via enzymatic reconstitution with isotopically labeled hemes, J. Am. Chem. Soc. 115 (1993) 12446–12458, https://doi.org/10.1021/ja00079a028.

[15] Han S. Czernuszewicz, R.S., Kimura T., Adam M.W.W., Spiro T.G. *Fe2S2 Protein Resonance Raman Spectra Revisited: Structural Variations among Adrenodoxin, Ferredoxin, and Red Paramagnetic Protein*, J. Am. Chem. SOC. pp. 3505-3511, https://doi.org/10.1021/ja00192a003.

[16] A. Krige, M. Sjöblom, K. Ramser, P. Christakopoulos, U. Rova, On-Line Raman Spectroscopic Study of Cytochromes' Redox State of Biofilms in Microbial Fuel cells, Mol. [Internet] 24 (3) (2019). ⟨https://urn.kb.se/resolve?urn=urn:nbn:se:ltu:diva-73003⟩ (Available from).

[17] K. Charubin, E.T. Papoutsakis, Direct cell-to-cell exchange of matter in a synthetic Clostridium syntrophy enables CO2 fixation, superior metabolite yields, and an expanded metabolic space, Metab. Eng. 52 (2019) 9–19, https://doi.org/10.1016/j.ymben.2018.10.006.

[18] P.H.C. Eilers, A perfect smoother, Anal. Chem. 75 (14) (2003) 3631–3636, https://doi.org/10.1021/ac034173t.

[19] A. Cao, et al., A robust method for automated background subtraction of tissue fluorescence, J. Raman Spectrosc. 38 (9) (2007) 1199–1205, https://doi.org/10.1002/jrs.1753.

[20] B. Kamlage, A. Boelter, M. Blaut, Spectroscopic and potentiometric characterization of cytochromes in two *Sporomusa* species and their expression during growth on selected substrates, Arch. Microbiol 159 (1993) 189–196, https://doi.org/10.1007/BF00250281.

[21] M. Visser, M.M. Pieterse, M.W.H. Pinkse, B. Nijsse, P.D.E.M. Verhaert, W.M. de Vos, P.J. Schaap, A.J.M. Stams, Unravelling the one-carbon metabolism of the acetogen Sporomusa strain An4 by genome and proteome analysis, Environ. Microbiol. 18 (2016) 2843–2855, https://doi.org/10.1111/1462-2920.12973.